Journal of Electrical Engineering & Technology
https://doi.org/10.1007/s42835-024-01945-1

ORIGINAL ARTICLE

A Two-Layer Planning Method for Distributed Energy Storage with Multi-point Layout in High Photovoltaic Penetration Distribution Network

Yukai Wei[1] · Bo Zhao[1] · Juan Hu[2] · Xiaolong Xiao[3] · Mingming Shi[3] · Qi Zhou[3]

Received: 25 June 2023 / Revised: 18 January 2024 / Accepted: 26 May 2024

Abstract
In the planning of energy storage system (ESS) in distribution network with high photovoltaic penetration, in order to fully tap the regulation ability of distributed energy storage and achieve economic and stable operation of the distribution network, a two-layer planning method of distributed energy storage multi-point layout is proposed. Combining with the operation characteristic model of energy storage battery (ESB), a multi-point energy storage collaborative operation strategy considering the service life of ESB is proposed. A planning-operation two-layer model is constructed, in which the outer layer considers the total cost of ESS planning to determine the layout point number and capacity of ESS, and the inner layer focuses on the utilization rate of ESB and the operation stability of distribution network. The hybrid particle swarm optimization and non-dominated sorting genetic algorithm is used to solve the planning and operation results of distributed energy storage multi-point layout. Example analysis shows that after configuring a multi-point layout ESS, the total planning cost decreases by 20.25%, the utilization rate of ESB increases to over 50%, and the voltage fluctuation and loss rate of the distribution network decrease by 19.09% and 11.76%, respectively.

Keywords Distribution network · Distributed energy storage · Multi-point layout · Operation strategy · Site selection and capacity determination

1 Introduction

With the proposal of China's "dual-carbon" goal, accelerating the construction of a new power system primarily based on new energy is an inevitable trend, while continuously increasing the proportion of new energy in traditional energy is a strategic choice for China and even the world [1–5]. However, as the installed capacity of distributed generation (DG) continues to increase, its volatility and uncertainty pose higher requirements for the power system's absorption capacity and scheduling operation [6, 7]. Among them, energy storage system (ESS) with flexible charging and discharging capabilities have become key to building a new power system [8]. Therefore, how to reasonably configure the ESS of a high-penetration new energy distribution network, such as different access positions will change the system's flow distribution, affecting network losses and system voltage levels; excessive capacity will make the system uneconomical, and insufficient capacity cannot meet the demand under different scenarios; has become an urgent problem to be solved [9–11].

Several scholars have made progress in the optimization and configuration of ESS in distribution network [12]. Established a new model for calculating the life cycle of energy storage, considering the shortcomings in the lifespan and economic aspects, to achieve the optimal configuration and operation of ESS [13]. Established a bi-objective model for optimizing the ESS distribution network with the objectives of minimizing the total cost and voltage fluctuation, which reduces the operating cost of the distribution network [14]. Optimized the installation capacity and charging-discharging

✉ Bo Zhao
lingshanisland@126.com

Yukai Wei
1424040820@qq.com

1 Beijing Information Science and Technology University, Beijing, China

2 China Electric Power Research Institute, Beijing, China

3 State Grid Jiangsu Electric Power Co., Ltd., Research Institute, Nanjing, China

Published online: 20 June 2024

control strategies of user-side energy storage by considering factors such as peak shaving benefits, demand defense benefits, and life cycle cost in the objective function of energy storage optimization [15]. Established a multi-objective site selection and rated capacity model for ESS active distribution networks based on three aspects: vulnerability indicators of power grids, active network loss, and rated capacity of ESS, which effectively improves the operational economy of the power grid [16]. Established an energy storage capacity optimization model with load shedding rate and energy overflow ratio as evaluation indicators, and analyzed two modes of energy storage configuration: separate configuration and photovoltaic energy storage collaborative configuration, which improves the fluctuation of energy storage output [17]. Constructed a cluster energy storage economic model to improve the absorption of distributed energy sources and determine the optimal timing of energy storage output in each node of the distribution network. These references discuss the application of ESS distribution networks from the perspectives of planning costs, peak shaving and voltage regulation, and promoting the integration of renewable energy sources, but they all focus on the fixed number of ESS site selection and rated capacity problems under a single typical load scenario.

As for the optimal layout of ESS in distribution network under different demand scenarios, [18] established an economic model for reducing power grid loss, improving the reliability of distribution networks, and profiting from energy storage, and planned the capacity of ESS accordingly [19]. Described the impact of different energy storage locations and capacities on the wind power integration capacity of the system by establishing a correlation analysis model between the configuration of energy storage and wind power integration capacity [20]. Dynamically planned the nodes and rated capacity of ESS by constructing an energy storage distribution center in the distribution network area, but this significantly increased the investment cost [21]. Mainly constructed a long-term uncertainty-adaptive ESS planning and operation model from the perspective of economic cost and energy storage capacity, but did not optimize the optimal number and location of ESS. Moreover, in solving the double-layer planning model with coupled internal and external parameters, many scholars focused on converting it into a second-order cone programming model [20] or using the Karush–Kuhn–Tucker (KKT) method [22, 23], which is complex and has biased calculation efficiency, and there are also problems with the difficulty of model conversion. Meanwhile, in using intelligent optimization algorithms to solve the model, many scholars improved the particle swarm algorithm (PSO) to transform the double-layer model into a multi-objective function processing model [4, 24], but there are still shortcomings in the application methods for directly and effectively solving the double-layer model.

In summary, there is currently insufficient in-depth research on seeking the optimal number of distributed energy storage layout points through dynamic planning in distribution network with high penetration PV. There are deficiencies in research on whether distributed energy storage planning methods in fixed scenario are suitable for other seasonal scenarios.

Therefore, in order to fully tap the regulation ability of distributed energy storage, improve the adaptability in different seasonal scenarios, and achieve economic and stable operation of distribution network, a two-level planning method for multi-point layout of distributed energy storage is proposed.

The Sect. 1 introduces the research background of this article and analyzes the main hot topics and shortcomings of current research. In the Sect. 2, a model for PV access to the distribution network and an operation model for ESB were established, and a collaborative operation strategy considering battery life was proposed. Considering both the planning cost of ESS and the stability requirement of distribution network, a two-layer model of planning-operation for multi-point layout was constructed. In the Sect. 3, to reduce the difficulty of solving the two-layer model, a hybrid approach of particle swarm optimization and non-dominated sorting genetic algorithm (PSO-NSGA-III) was utilized. This section provided a detailed introduction to the solving process of the hybrid algorithm. The Sect. 4 validated the effectiveness of the model and algorithm by simulating different scenarios on the IEEE-33 distribution network. The Sect. 5 is the conclusion of this article.

2 Distribution Network and ESS Model Construction

2.1 Distributed PV Access to Distribution Network Model

Taking Fig. 1 as an example, distributed photovoltaic (PV) are connected to a distribution network model with a radial feeder with n nodes. It is assumed that at time t, the load at node i is $P_{li}+jQ_{li}$, $i=1, 2,\ldots,$ n.

The voltage drops and impedance branch loss of node i at time t is given by Eq. (1), where $U_{i(t)}$ is the voltage at the

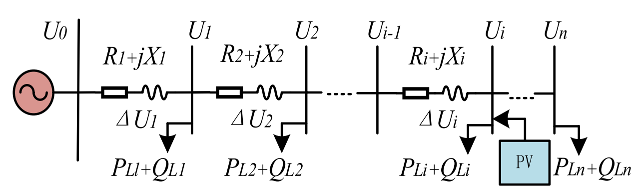

Fig. 1 Distributed PV access distribution network model

end of branch i at time t, and R_i and X_i are the resistance and reactance of branch i.

$$\begin{cases} \Delta U_{i,(t)} = \dfrac{P_{Li}R_i + Q_{Li}X_i}{U_{i,(t)}} \\ P^{loss}_{i,(t)} = \dfrac{R_i(P^2_{Lj} + Q^2_{Lj})}{U^2_{i,(t)}} \end{cases} \tag{1}$$

After adding a PV power source with a power of $P^{PV}{}_{i,(t)}$ at the end of the line of node i at time t. The voltage drops and impedance branch loss at node i at that time are:

$$\begin{cases} \Delta U_{i,(t)} = \dfrac{(P_{Li} - P^{PV}_{i,(t)})R_i + Q_{Li}X_i}{U_{i,(t)}} \\ P^{loss}_{i,(t)} = \dfrac{R_i((P_{Li} - P^{PV}_{i,(t)})^2 + Q^2_{Lj})}{U^2_{i,(t)}} \end{cases} \tag{2}$$

According to Eq. (2), when the output power of the PV system $P^{PV}{}_{i,(t)}$ is less than the end load P_{Li} at time t, all the electrical energy generated by the PV system is consumed by the load. Increasing $P^{PV}{}_{i,(t)}$ can reduce the voltage drop $\Delta U_{i,(t)}$ and power loss $P^{loss}{}_{i,(t)}$. When $P^{PV}{}_{i,(t)}$ is greater than P_{Li}, $\Delta U_{i,(t)}$ first decreases in the forward direction, then increases in the reverse direction, that is, the end voltage increases, even exceeding the initial voltage, while the losses also increase. Therefore, in a distribution network with high PV penetration, due to the intermittency and fluctuation of PV energy, ESS need to be installed to improve the flow of the distribution network, enhance the power quality, and better integrate new energy sources.

2.2 Energy Storage Battery Model

The remaining capacity of an energy storage battery (ESB) is generally represented by the State of Charge (SOC). During the charging and discharging process of the ESB, the SOC and the charging and discharging power model are given by the following equation.

$$\begin{cases} S_{SOC,(t)} = \max\left\{ S_{SOC,(t-\Delta t)} - \dfrac{P^{BESS}_{(t)} \cdot \Delta t}{E^{BESS}\lambda_{dis}}, S_{SOC,\min} \right\} \\ S_{SOC,(t)} = \min\left\{ S_{SOC,(t-\Delta t)} + \dfrac{P^{BESS}_{(t)} \cdot \Delta t \cdot \lambda_c}{E^{BESS}}, S_{SOC,\max} \right\} \\ S_{SOC,s} = S_{SOC,e} \\ \left|P_{\min^{BESS}}\right| \le \left|P^{BESS}_{(t)}\right| \le \left|P_{\max^{BESS}}\right| \\ E^{BESS} = \beta P^{BESS} \end{cases} \tag{3}$$

where $P_{(t)}{}^{BESS}$ represents the charging and discharging power of ESB at time t, with a positive value for discharging and a negative value for charging. $S_{SOC,(t)}$ and $S_{SOC,(t\text{-}\Delta t)}$ represent the remaining energy of ESB at time t and $t\text{-}\Delta t$, respectively. λ_c and λ_{dis} represent the charging and discharging efficiency. E^{BESS} represents the rated capacity. $P_{max}{}^{BESS}$ and $P_{min}{}^{BESS}$ represent the upper and lower limits of the charging and discharging power, respectively. $S_{SOC,max}$ and $S_{SOC,min}$ represent the upper and lower limits of the charging and discharging depth, respectively. $S_{SOC,s}$ and $S_{SOC,e}$ represent the SOC at the start and end of the operating cycle, respectively. β represents the energy rate of the ESB, and Δt represents the time interval.

2.3 Multi-Point Collaborative Operation Strategy Considering Battery Life

Based on the characteristics of the ESB, there is a maximum limit to the number of charge and discharge cycles that the battery can undergo during its entire lifespan. In order to avoid frequent charge and discharge cycles that may affect the life of the ESB, it is necessary to develop a charging and discharging strategy for the ESS within a certain operating period to reduce unnecessary charge and discharge cycles. The traditional strategy is to design the time-of-use pricing intervals for the ESS based on the power difference between the PV system and the load, which can be referred to in reference [25]. Based on the multi-point energy storage planning, this paper proposes a collaborative operation strategy for multi-point energy storage considering battery life, which reduces the frequency of charging and discharging of the energy storage system (ESS) and thus reduces the loss of the energy storage battery to achieve optimal operation. The objective function f is combined with the charging and discharging frequency of the ESB ($R^{BESS}{}_{fre}$) to satisfy $f = min\ \{R^{BESS}{}_{fre}\}$.

- Firstly, the average charging and discharging power of the ESS during its operation cycle is compared with the average net load of the distribution network system at each time. If it does not exceed the specified range, the charging and discharging interval strategy of the ESB remains unchanged. If it exceeds the specified range, the number of exceeded intervals is calculated.
- Then, the ESB with the highest frequency of charging and discharging in the ESS is identified, and its interval is shifted to the valley period of the time-of-use pricing interval. The size of the interval shift is the number of calculated intervals in step 1, and the charging and discharging power of the ESB is determined according to the new interval.

- Repeat the above steps to obtain the minimum value of the objective function *f*.

2.4 The Outer Planning Model

Citations the outer planning model primarily considers the economic costs of ESS planning for the distribution network.

(1) Objective Function

ESS typically consist of storage units, power conversion system (PCS), and auxiliary equipment.

$$\begin{cases} f_1 = \min\left\{C_{plan}\right\} = \min\left\{C_b + C_p + C_f\right\} \\ C_b = \frac{1}{365} \cdot \frac{\gamma(1+\gamma)^{yBESS}}{\gamma(1+\gamma)^{yBESS}-1} \cdot C_b^{BESS} \cdot (\sum_{r=1}^{NUM} E_{in,r}^{BESS}) \\ C_p = \mu C_b + \sum_{r=1}^{NUM} (k_{re}^{BESS} \cdot E_{in,r}^{BESS}) \\ C_f = \sum_{r=1}^{NUM} (\varepsilon E_{in,r}^{BESS} + \omega \left| P_{in,r,\max}^{BESS} \right|)) \end{cases} \tag{4}$$

where C_{plan} represents the total planning cost of the ESS in the distribution network. C_b、 C_p and C_f represent the investment and construction cost of energy storage (converted to daily investment and construction cost matching the operation period), operation and maintenance cost (considering the long-term partial capacity decay of ESB and the need for replacement), and auxiliary equipment cost, respectively. γ and y^{BESS} represent the discount rate and service life of energy storage. C_b^{BESS} represents the unit capacity investment and construction cost of energy storage. $E^{BESS}{}_{in,r}$ and $P^{BESS}{}_{in,r,max}$ represent the layout capacity of the *r*-th energy storage and the maximum charging and discharging power during the operation period, respectively. *NUM* represents the total number of energy storage layouts. μ represents the conversion ratio of operation and maintenance cost, which is selected as 10% based on reference [15] and engineering experience. $k^{BESS}{}_{re}$ represents the replacement rate of ESB. ε and ω represent the capacity coefficient and power coefficient of auxiliary equipment in the ESS.

(2) Constraint conditions

The planning model mainly considers constraints on the operating power of PV, the maximum number and location of energy storage layouts, and the characteristics of ESB.

Constraint on operating power of PV.

$$P_{j,(t),\min}^{PV} \le P_{j,(t)}^{PV} \le P_{j,(t),\max}^{PV} \tag{5}$$

where $P^{PV}{}_{j,(t),max}$ and $P^{PV}{}_{j,(t),min}$ respectively represent the upper and lower limits of the output value of PV installed at node *j* and time *t*.

Maximum layout number and position constraints for energy storage.

$$\begin{cases} \sum\limits_{i \in S_{SG}} S_{G,i} \le N_{num} \\ S_{G,r} \ne S_{G,r+1} \end{cases} \tag{6}$$

where S_{SG} represents the set of energy storage node to be installed. N_{num} represents the maximum layout total number of energy storage plans. $S_{S,r}$ represents the layout position of the *r*-th energy storage, and multiple energy storages cannot be laid out in the same position.

ESB characteristic constraints are shown in Eq. (3).

2.5 The Inner Operational Model

(1) The utilization rate of the ESB ($H^{BESS}{}_{con}$) is used to represent the potential of energy storage to improve the distribution network flow, and to characterize the frequency of charge and discharge that the ESB can reduce. The objective function f_2 can be expressed as:

$$\begin{cases} f_2 = max\left\{H_{con}^{BESS}\right\} = max\left\{1 - R_{fre}^{BESS}\right\} \\ H_{con}^{BESS} = \frac{\sum_{r=1}^{NUM} \sum\limits_{t \in S_{ESS}} S_{ESS(t)=0,r}}{T \cdot NUM} \end{cases} \tag{7}$$

where *T* represents the duration of statistical calculation cycle. S_{ESS} represents the collection of ESB charging and discharging power at all moments. $S_{ESS(t)=0,r}$ represents the *r*-th moment when the charging and discharging power is 0.

(2) One of the important indicators to measure the stability of the distribution network is the voltage fluctuation at nodes. As analyzed in Sect. 2.1, the penetration of high-penetration PV will exacerbate voltage fluctuation. Therefore, the daily voltage deviation index U_{exc} is selected to evaluate the ability of the ESS to improve voltage fluctuation, and the objective function f_3 can be expressed as:

$$\begin{cases} f_3 = min\left\{U_{exc}\right\} \\ U_{exc} = \frac{1}{T} \sum_{t=1}^{T} \sum_{i=1}^{N} \left(\frac{U_{i,(t)} - U_{i,(t)}^*}{\Delta U_{i,max}} \right)^2 \end{cases} \tag{8}$$

where *N* represents the number of load nodes. $U_{i,(t)}$ and U_i * represent the voltage and reference voltage of the *i*-th node at time *t*, respectively. $\Delta U_{i.max}$ is the maximum allowable deviation of the voltage at the *i*-th node.

(3) The network loss rate is an important economic indicator for assessing the operation level of a power system. Due to the high penetration rate of PV, the system network loss increases due to the occurrence of power generation inversion. Therefore, the network loss rate is selected as the indicator to evaluate the ability of energy storage configuration to reduce system network loss. The objective function f_4 can be expressed as:

$$\begin{cases} f_4 = min\{\eta_{P^{loss}}\} \\ \eta_{P^{loss}} = \frac{\sum_{t=1}^{T}\sum_{i}^{M} P_{i,(t)}^{loss}}{\sum_{t=1}^{T}\sum_{i}^{M}(P_{i,(t)}^{loss}+P_{i,(t)}^{load})} \times 100\% \end{cases} \tag{9}$$

where ${P_{i,(t)}}^{loss}$ and ${P_{i,(t)}}^{load}$ represent the line loss and end node load of branch i at time t, respectively. M is the total number of branches.

(4) Constraint conditions

The operational model mainly considers the power balance constraint, flow constraint, node voltage constraint, and line current constraint of the distribution network.

Power balance constraint.

$$\sum(P^{ES} + P^{PV} + P^{BESS}) = \sum(P^{load}+P^{loss}) \tag{10}$$

where P^{ES} represents the power supply of the distribution network. P^{PV} and P^{BEES} represent the grid-connected power of PV and energy storage respectively. P^{load} and P^{loss} represent the power consumption of the system and the active power loss of the system, respectively.

Power flow constraints [26].

$$\begin{cases} P_m - V_m \times \sum_{n=1}^{N} V_n(G_{mn}\cos\delta_{mn} + B_{mn}\sin\delta_{mn}) = 0 \\ Q_m - V_m \times \sum_{n=1}^{N} V_n(G_{mn}\sin\delta_{mn} + B_{mn}\cos\delta_{mn}) = 0 \end{cases} \tag{11}$$

where P_m and Q_m represent the active power and reactive power transmitted from node m, respectively. V_m and V_n and represent the voltages at node m and node n, respectively. G_{mn} and B_{mn} are the conductance and susceptance between node m and node n, respectively. δ_{mn} is the phase angle difference between node m and node n.

Node voltage constraints.

$$U_{i,\min} \le U_{i,(t)} \le U_{i,\max}, \forall i \in E \tag{12}$$

where $U_{i,max}$ and $U_{i,min}$ denote the upper and lower limits of the voltage amplitude at node i, respectively, and E represents the set of nodes in the power grid.

Line current constraints.

$$\left|I_{ij,(t)}\right| \le I_{ij,\max}, \forall (i,j) \in E \tag{13}$$

where $I_{ij,max}$ represents the maximum load flow between node i and j, and $I_{ij,(t)}$ represents the current of the line during time period t.

3 A Model Solution Method Based on PSO and NSGA-III Hybridization

3.1 PSO and NSGA-III Algorithm Hybridization

In the two-layer optimization model of this paper, the outer layer model is a single-objective problem and the inner layer model is a three-objective problem, which requires parameter transmission between the inner and outer levels during the solution process. Since converting a multi-objective problem into a single-objective problem by weighting requires normalization of parameters with different dimensions and it is difficult to obtain reasonable weighting coefficients, and the model in this paper is also difficult to transform into a second-order cone programming form. To this end, a hybrid algorithm of PSO and NSGA-III is employed to solve the bi-level multi-objective model. Among them, the advantages of PSO are fast convergence speed, fewer adjusted parameters [27], making it suitable for optimizing outer targets. NSGA-III is a novel multi-objective genetic algorithm proposed on the basis of fast non-dominated sorting genetic algorithm [28], which can well address the optimization problems with three or more objectives in an effective manner.

The solution steps of the algorithm are as follows.

1. The outer PSO initializes the velocity and position components of the outer population particles;
2. Based on the outer population, the inner NSGA-III selects, recombines, and mutates to generate an initial population P_t of size N, and then produces a population Q_t of size N. Using non-dominated sorting mechanism, N excellent individuals are selected from R_t ($R_t=P_t \cup Q_t$) to form a new generation of evolutionary population. R_t is divided into different non-dominated layers $F_{1,t}$, $F_{2,t}\cdots$, and the non-dominated sets with higher priority are preserved for the next generation;
3. When $|F_{1,t} \cup F_{2,t} \cup \cdots \cup F_{i-1,t}| < N$ and $|F_{1,t} \cup F_{2,t} \cup \cdots \cup F_{i,t}| > N$, $F_{i,t}$ is defined as a critical layer, and individuals are selected based on reference points to enter the next generation until the size of the offspring population is equal to N.

Selection based on reference points:

This method selects individuals to maintain population diversity and good distribution. Assuming that each target dimension is divided into p equal parts on the normalized hyperplane, the number of reference points H for M-dimensional targets is:

$$H = \frac{(M+p-1)!}{p!(M-1)!} \tag{14}$$

In 3-dimensional multi-objective optimization, if each objective is equally divided into 3 parts, 10 reference points with uniform distribution will be generated on the normalized hyperplane.

4. When the reference points are uniformly and widely distributed on the entire normalized hyperplane, the selected population will be widely and uniformly distributed on the true Pareto front. As the Pareto front solution set only provides non-dominated solutions for multiple objectives, corresponding methods need to be adopted to select the optimal solution from the Pareto solution set. Therefore, the entropy weight method (EWM) is used to select the optimal solution [29]
5. The optimal solution obtained from the inner NSGA-III is passed to the outer PSO to calculate the individual fitness function and update the outer population particles. The process of steps 2–5 is repeated until the optimal evaluation result (population iteration accuracy is less than 0.5%) is obtained or the maximum iteration times are reached.

The solution process is shown in Fig. 2

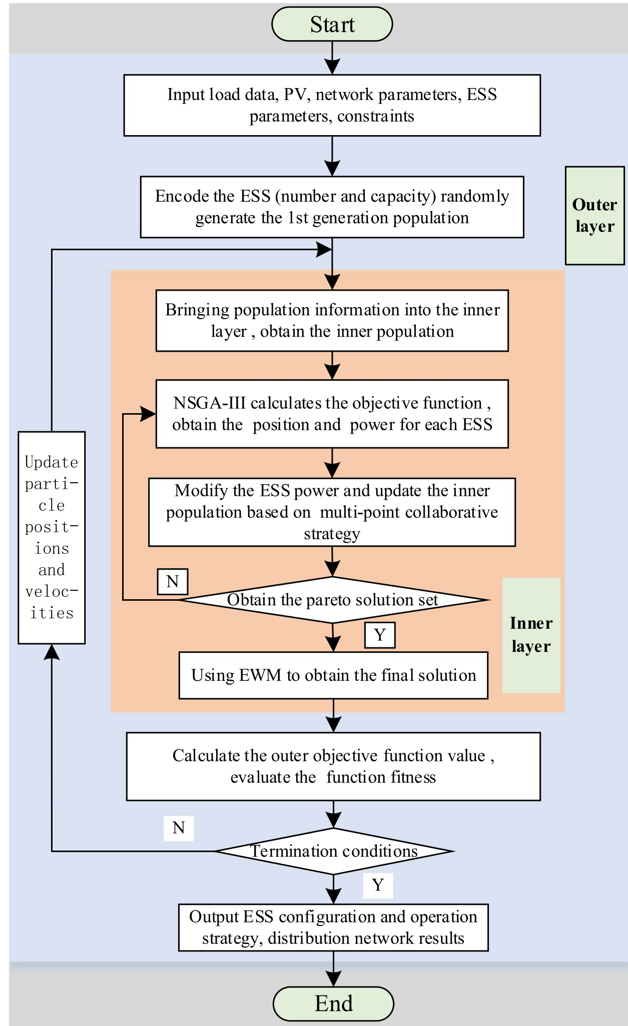

Fig. 2 Solution flowchart

3.2 The Relationship of the Two-layer Model

The relationship between the inner layer and outer layer of the two-layer model is shown in Fig. 3 the outer layer determines the layout points and capacity plans of the ESS. The inner layer solves the charging and discharging power, layout location, and collaborative operation strategy of each ESB.

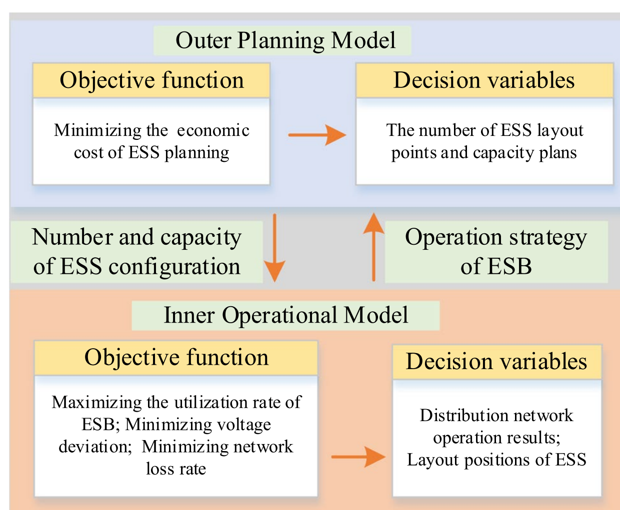

Fig. 3 The relationship of the two-layer model

4 Simulation Analysis

4.1 Simulation Setup

The IEEE-33 distribution network is selected as the test system. The total active power load of the system is 3715 kW (baseline value), with a rated voltage of 12.66 kV. The allowable range of voltage deviation is 11.90–13.42 kV (0.94 p.u–1.06 p.u), and the maximum transmission current of the line is 0.55 kA. The topology structure is shown in Fig. 4 In the network, the total installed capacity of PV

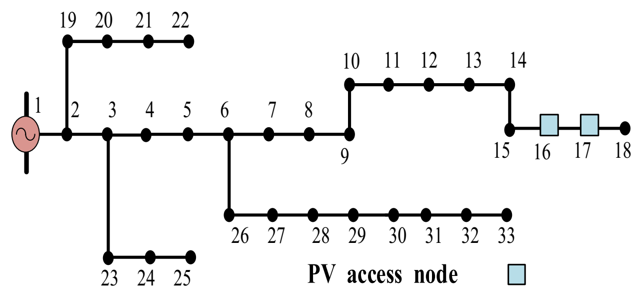

Fig. 4 IEEE-33 system

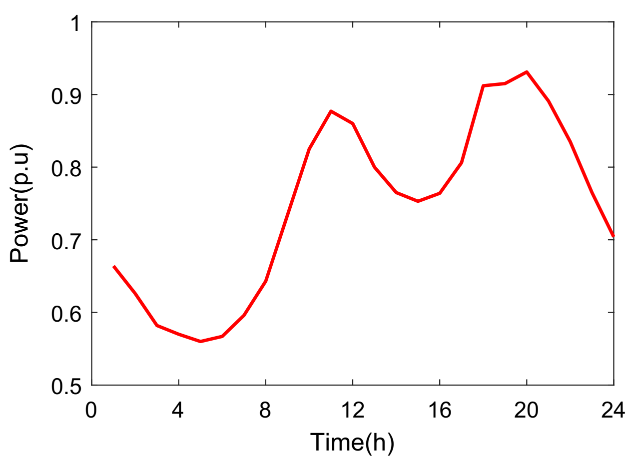

Fig. 5 Typical daily load curve

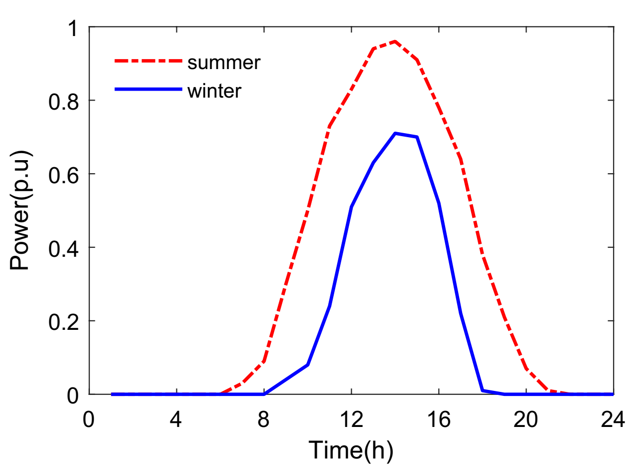

Fig. 6 Typical daily output curve of PV

is 2.5 MW, accounting for 36.5% of the total daily load demand, and the access points are at node 16 and 17. The typical daily load curve, typical daily PV summer and winter output prediction curves of the system are shown in Figs. 5and 6 respectively. The parameters of the ESB are shown in Table 1.

Table 1 Energy storage battery parameters

λ_c	90%	μ	10%
λ_{dis}	90%	y^{BESS}	15
β	0.25C	k^{BESS}_{re}	5%
ε	0.25	γ	6.5%
ω	0.18	Initial SOC	50%
C_b^{BESS}	3800￥/(kW h)	$[S_{SOC,min}\ S_{SOC,max}]$	[0.1 0.9]

Firstly, based on the summer typical daily load demand and PV output, the following four scenarios are set up for comparative analysis.

Scenario 1: Access to PV power without considering ESS.

Scenario 2: Considering the ESS without considering multi-point layout.

Scenario 3: Considering the multi-point layout without considering the coordinated operation strategy.

Scenario 4: Considering the multi-point layout and coordinated operation strategy.

4.2 Model Calculation Results

Based on the bi-level programming model, the PSO-NSGA-III are used for calculation. The planning schemes and costs for the four scenarios are shown in Table 2; the utilization rate of ESB, system voltage deviation index, and network loss rate results are shown in Table 3. The fitness iteration curves of the outer-layer function and the Pareto frontier solution sets for each scenario are shown in Figs. 7and 8.

Comparing the results of scenarios 2, 3, and 4 with scenario 1, it can be seen that configuring ESS can effectively improve voltage fluctuation and reduce network loss in the distribution network. It reduced the voltage deviation index by 20.61%, 17.27%, and 19.09% respectively, and reduced the network loss rate by 11.19%, 10.04%, and 11.76%. The improvement effect is significant. Comparing the results of scenario 3 with scenario 1 and 2, it is found that the configuration of the energy storage layout as three points is the optimal result, which reduces the total planning cost by 15.50% and improves the utilization rate of ESB by 33.33%. Comparing the results of scenario 3 and 4, it is found that after using a collaborative operation strategy for multi-point ESB, the number of charge and discharge cycles of the ESB is further reduced, the utilization rate of the ESB is increased by 69.70%, and the energy storage capacity is reduced.

Therefore, combining the results of scenario 4 with Fig. 5, it can be seen that the multi-point layout configuration method considering collaborative operation strategy solves the problem of severe voltage fluctuation and increased network loss caused by high PV penetration in the distribution network, which once again verifies the conclusion that

Table 2 Planning schemes and planning costs for each scenario

Scenario	Energy storage battery		Cost planning			
	Node	Capacity (kW h)	C_b (10,00¥)	C_p (10,00¥)	C_f (10,000¥)	C_{plan} (10,000 ¥)
1	–	–	–	–	–	–
2	14	8364	0.926	0.098	0.175	1.200
3	15, 22, 17	2700, 1198, 2684	0.720	0.150	0.144	1.014
4	18, 23, 17	2651, 849, 2621	0.678	0.141	0.138	0.957

Table 3 Total energy storage capacity and system operation results for each scenario

Scenario	Total capacity (kW h)	The utilization rate	Voltage deviation index	Loss rate (%)
1	–	–	33.0	6.97
2	8364	0.33	26.2	6.19
3	6582	0.44	27.3	6.27
4	6121	0.56	26.7	6.15

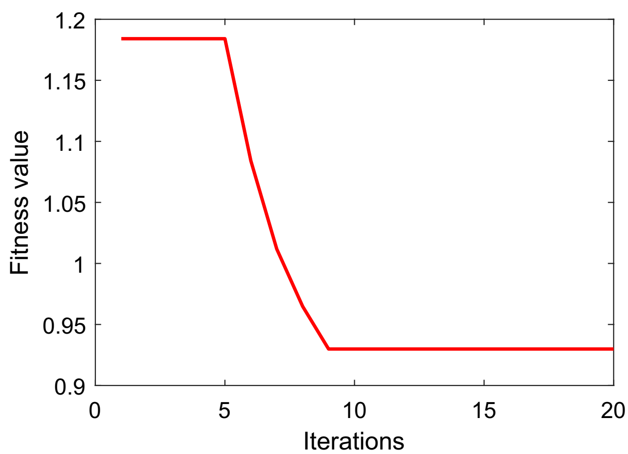

Fig. 7 Iterative curve of outer function fitness

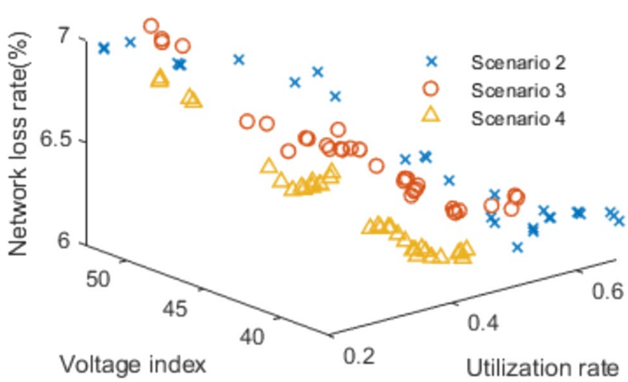

Fig. 8 Pareto frontier solution set for each scenario

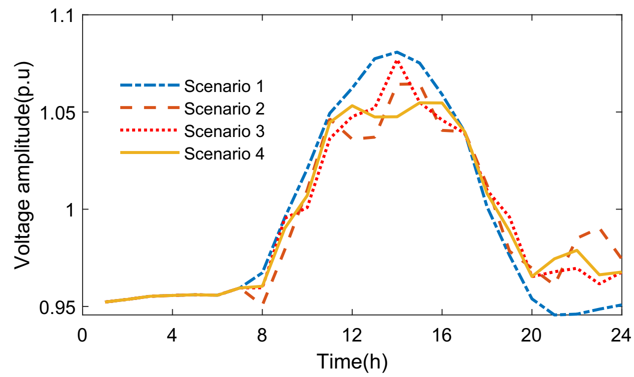

Fig. 9 Voltage variation for 24 h

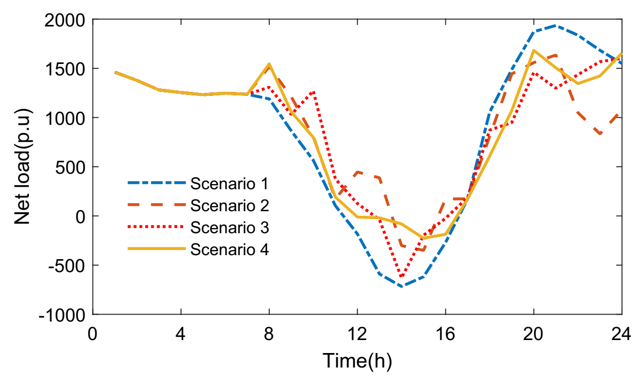

Fig. 10 Net load curve of each scenario system

configuring ESS can improve the system to consume new energy. Moreover, compared with the single-point configuration, the multi-point layout method not only achieves better improvement in the operation of the distribution network but also significantly reduces the total cost of ESS configuration.

The comparison of the voltage changes in the distribution network over 24 h for each scenario is shown in Fig. 9. Under scenario 4, ESS has the best effect on improving node voltage, reducing the original overvoltage value of about 1.08 p.u to about 1.05 p.u, and also raising the voltage during the 20:00–24:00 period (about 0.94 p.u to about 0.96 p.u), making the power supply voltage within the required range. The comparison of the net load curves in each scenario in Fig. 10 shows that when the ESS is configured with a

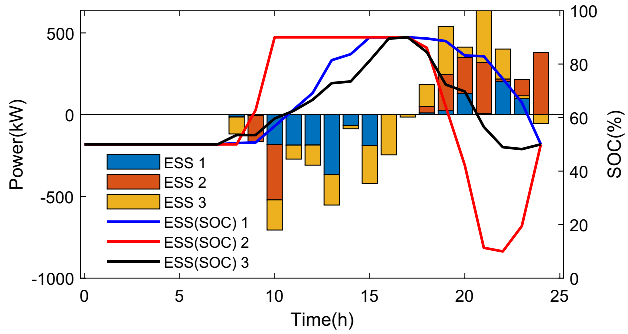

Fig. 11 Power and SOC in scenario 3

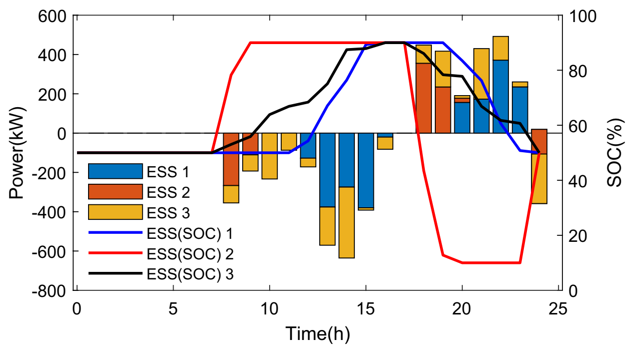

Fig. 12 Power and SOC in scenario 4

multi-point layout (scenario 4), it can better consume PV energy and balance the load.

The charging and discharging power and SOC in scenario 3 and 4 are shown in Figs. 11 and 12 respectively. Compared with scenario 3, the SOC trend in scenario 4 is similar, both charging during the peak period of PV output and discharging during the peak period of load, but the charging and discharging frequency in scenario 4 is significantly reduced. This is because after using a collaborative operation strategy for multi-point, effective power complementarity is formed between the ESB. For example, ESS 2 quickly discharges at high power from 17:00 to 20:00, reducing the number of discharges of ESS 1 and shortening the charge and discharge interval of ESS 1, thereby reducing the overall frequency of charge and discharge of the ESS and improving their utilization rate.

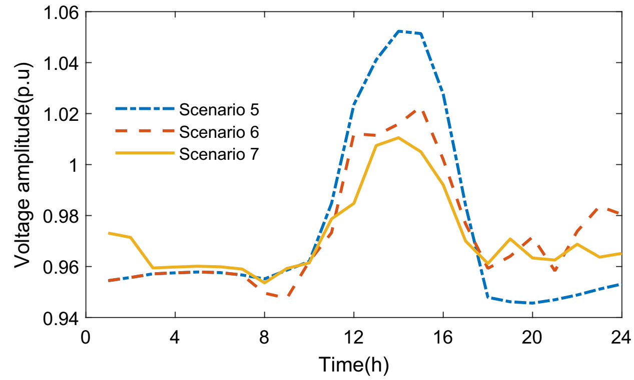

Fig. 13 Voltage variation for 24 h

4.3 Validation Analysis

To further investigate the applicability and effectiveness of the multi-point layout and its coordinated operation strategy proposed, Scenario 5, 6, and 7, are set up. Scenario 5 examines the performance of the distribution network without ESS during winter PV output and load demand. Scenario 6 and 7 analyze the impact of the ESS configuration scale on the winter distribution network operation performance based on the ESS configuration scale of Scenario 2 and 4, respectively. The system operation results under the three scenarios are shown in Table 4. The voltage variation and system net load curves for each scenario are shown in Figs. 13 and 14, respectively. The charging and discharging power and SOC in Scenario 6 and 7 are illustrated in Figs. 15 and 16, respectively.

The above results show that scenarios 6 and 7 respectively reduced the voltage deviation index by 15.48% and 16.96%; reduced the network loss rate by 11.22% and 13.90%; and increased the utilization rate of ESB by 51.52% compared to scenario 6. Therefore, when facing winter PV output and load demand, although the ESS scale configuration was based on summer scenarios, multi-point still has advantages over single-point configuration. From Fig. 14 combined with Figs. 15 and 16, it can be seen that scenario 7 showed a small-scale peak-shifting phenomenon in the net load curve after ESS regulation. This is because the winter PV output interval is shortened, and the coordinated operation strategy of using

Table 4 System operation results for each scenario

Scenario	Energy storage battery			Distribution network	
	Node	Capacity (kW h)	The utilization rate	Voltage deviation index	Loss rate(%)
5	–	–	–	33.6	5.97
6	14	8364	0.33	28.4	5.30
7	18, 23, 17	2651, 849, 2621	0.50	27.9	5.14

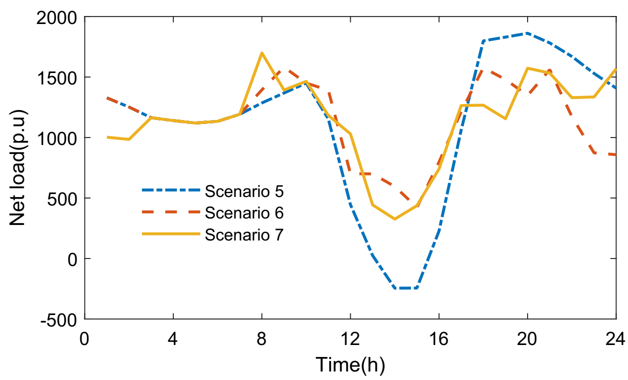

Fig. 14 Net load curve of each scenario

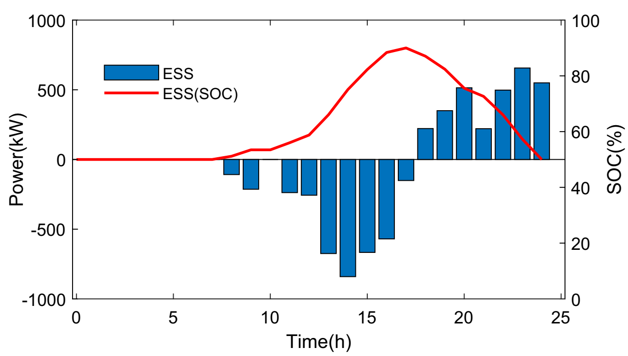

Fig. 15 Power and SOC in scenario 6

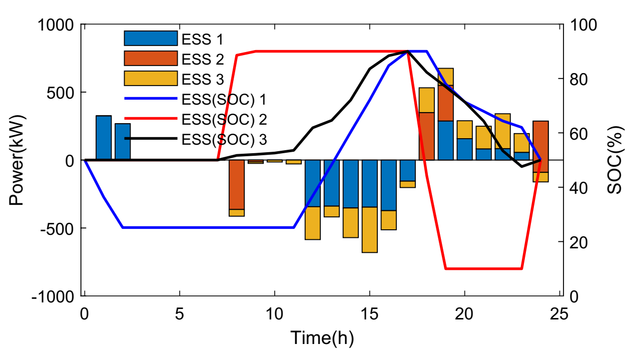

Fig. 16 Power and SOC in scenario 7

multi-point optimizes the balance between PV output and load demand, further reducing the voltage fluctuation and network loss rate of the system.

5 Conclusion

This paper proposes a planning-operation two-layer model for distributed energy storage with multi-point layout. The conclusions are as follows:

- The multi-point layout of distributed energy storage is more helpful to enhance the ability of power distribution network to consume new energy and improve the economic efficiency and stability of the system. The total planning cost has been reduced by 20.25%, the voltage deviation of the distribution network has been reduced by 19.09%, and the network loss rate of the system has been reduced from 6.97 to 6.15%.
- Compared with the utilization rate of ESB in a single-point layout, the utilization rate in a multi-point layout scenario is increased to over 30%. When considering the collaborative operation strategy of multi-point ESS, increase the utilization rate to over 50%. This significantly reduces the charging and discharging frequency of ESB and improves their service life.
- When using the scale of energy storage layout configuration obtained from a single season, when facing PV output and load demand scenario of different seasons, the multi-point layout of energy storage still has stronger regulation ability compared to single point configuration. The multi-point layout method enhances the coordination of the system.
- The PSO-NSGA-III hybrid algorithm proposed in this article is suitable for solving multi-objective optimization problem. It can effectively find the optimal number of distributed energy storage layout point and capacity configuration scheme for the high PV penetration distribution network, and solve the corresponding ESB charging and discharging strategy.

Acknowledgements This work was supported by State Grid Jiangsu Electric Power Co technology projects (J2022040).

Declarations

Conflict of interest On behalf of all authors, the corresponding author states that there is no conflict of interest.

References

1. Xiangjun LI, Huimeng MA, Qian J (2022) Review of energy storage configuration technology on renewable energy side. Electr Power 55(01):13–25
2. Yang Y, Bremner S, Menictas C et al (2018) Battery energy storage system size determination in renewable energy systems: a review. Renew Sustain Energy Rev 91:109–125
3. Gehao S, Yong Q, Lingen L et al (2021) Key technologies and application prospects for operation and maintenance of power equipment in new type power system. High Voltage Eng 47(9):3072–3084
4. Dehghani-Sanij AR et al (2019) Study of energy storage systems and environmental challenges of batteries. Renew Sustain Energy Rev 104:192–208

5. Chen H et al (2021) Optimal energy management strategy for an islanded microgrid with hybrid energy storage. J Electrical Eng Technol 16(3):1313–1325
6. Valencia A, Hincapie RA, GALLEGO RA (2021) Optimal location, selection, and operation of battery energy storage systems and renewable distributed generation in medium-low voltage distribution networks. J Energy Storage 2021(34):102158
7. Yan QM, Mu JH, Ma YX et al (2022) Review of distributed energy storage application mode and optimal configuration. Electr Power Eng Technol 41(02):67–74
8. Sun X, Sheng Y, Wu C et al (2023) Comprehensive evaluation of interval equalization of power quality in active distribution network based on CVAE-TS. Electr Eng Technol. https://doi.org/10.1007/s42835-023-01528-6
9. Elnozahy A et al (2021) Optimal economic and environmental indices for hybrid PV/Wind-based battery storage system. J Electrical Eng Technol 16(6):2847–2862
10. Luo J, Shi L, Ni Y (2018) A solution of optimal power flow incorporating wind generation and power grid uncertainties. IEEE Access 6:19681–19690. https://doi.org/10.1109/ACCESS.2018.2823982
11. Maurya R, Prakash S, Singh AKJ (2023) Challenges, configuration, control, and scope of DC microgrid systems: a review. Electr Eng Technol 18:1655–1674. https://doi.org/10.1007/s42835-022-01304-y
12. Wang Z, Chen J, Zhu J et al (2021) Optimal configuration and operation strategy of energy storage considering cycle life[J]. Electr Power Automation Equip 41(10):75–81
13. Zhao J, Su J, Pan F et al (2022) Dual objective optimization planning of distributed energy storage for active distribution network considering photovoltaic fluctuations. Renew Energy Resour 40(11):1546–1553
14. Bin GUO, Jie XING, Fei YAO et al (2022) Optimal configuration of user-side hybrid energy storage based on bi-level programming model. Energy Storage Sci Technol 11(02):615–622
15. Yan Q, Dong X, Mu J et al (2022) Energy storage optimization of active distribution network based on improved multi-objective particle swarm optimization algorithm. Power Syst Prot Control 50(10):11–19
16. Li J, Tan Y, Wang H et al (2022) Research on configuration optimization of energy storage system in distribution network and optical storage microgrid. High Voltage Engi 48(05):1893–1902
17. Li C, Dong Z, Li J et al (2021) Optimal control strategy of distributed energy storage cluster for prompting renewable energy accommodation in distribution network. Automation of Electr Power Syst 45(23):76–83
18. Damavandi MG, Marti JR, Krishnamurthy V (2018) A methodology for optimal distributed storage planning in smart distribution grids. IEEE Trans Sustainable Energy 9(2):729–740
19. Cheng Y, Chen X (2022) Analysis on influence of energy storage on accommodation capability of wind power based on source load storage interaction. Automation Electr Power Syst 46(13):84–93
20. Shang L, Wei B, Wang W et al (2020) A planning method of dynamic energy storage configuration in an active distribution network. Power Syst Protection Control 48(17):84–92
21. Bin N, Shufeng D, Kunjie T et al (2020) Optimal configuration of energy storage in pv-storage microgrid considering demand response and uncertainties in source and load. Power Syst Technol 48(17):84–92
22. Xie Y, Luo Y, Li Z et al (2022) Optimal allocation of shared energy storage considering the economic consumption of microgrid new energy. High Voltage Eng 48(11):4403–4413
23. Marcos T, Ahmad RJ, Lázuli F et al (2023) Robust energy management in isolated microgrids with hydrogen storage and demand response. Appl Energy 345(2023):121319
24. Liu Z, Yu P, Li J (2023) Planning of distributed generation and generalized energy storage in distribution network considering operation characteristics. Electr Power Automation Equip 43(03):72–79
25. Wang S, Wang H, Zhao Q et al (2023) Optimization method of time-of-use electricity price for photovoltaic hosting capacity improvement of distribution network. Automation Electr Power Syst 47(10):38–46
26. Ahmad AAL, Sirjani R, Daneshvar S (2020) New hybrid probabilistic optimization algorithm for optimal allocation of energy storage systems considering correlated wind farms. J Energy Storage 29:101335
27. D Bratton J Kennedy 2007 Defining a standard for particle swarm optimization 2007 IEEE swarm intelligence symposium honolulu HI USA 120 127 https://doi.org/10.1109/SIS.2007.368035
28. Deb K, Jain H (2014) An Evolutionary many-objective optimization algorithm using reference-point-based nondominated sorting approach part i: solving problems with box constraints. IEEE Trans Evol Comput 18(4):577–601
29. Li W et al (2008) Analysis of multiple objective decision methods based on entropy weight. Asia Workshop on Computational Intelligence and Industrial Application proceedings, vols 1–3. pp 917–920

Yukai Wei He received a B.S. degree in electrical engineering from Henan University of Technology, China. He is currently pursuing a master's degree at Beijing Information Science and Technology University. His research interests include distribution automation and distributed energy storage configuration and control technology.

Bo Zhao He received B.S. and M.S. degrees in electrical engineering from Beijing University of Aeronautics and Astronautics and received Ph.D. degrees in electrical engineering from the China Electric Power Research Institute. He has worked at Beijing Information Science & Technology University since 2018 and is now a researcher/professor-level senior engineer. His current research interests include the analysis and control of new energy and energy storage and the protection and control of microgrids.

Juan Hu She received B.S. degrees and M.S degrees from Hunan University. She works in the China Electric Power Research Institute since 2003 and now as a senior engineer. Her current research interest includes energy storage, power electronics and flexible AC transmission.

Xiaolong Xiao He received a B.S. degree in electrical engineering from Wuhan University of Science and Technology, China. He received an M.S. degree in electrical engineering from the State Grid Electric Power Research Institute. His research interests are distribution automation, DC distribution technology, distributed generation and microgrid technology.

Mingming Shi He received B.S. and Ph.D. degrees in electrical engineering from the Nanjing University of Aeronautics and Astronautics, China. His research focuses on distributed generation systems and power quality analysis.

Qi Zhou He received B.S. and M.S. degrees in electrical engineering from the Shandong University, China. His research focuses on energy storage and power electronics technology.